

## Enhancing corrosion resistance of stainless steel 316L implants: Hydroxyapatite coating via DC and AC-DC voltage electrochemical deposition

Alivia Nurul Avivin<sup>1\*</sup>, Prabowo Puranto<sup>2</sup>, Maymunah Zilallah<sup>3</sup>, Muhammad Prisla Kamil<sup>2</sup>, Diah Ayu Fitriani<sup>2</sup>, Kusuma Putri Suwondo<sup>2</sup>, Muhammad Kozin<sup>2</sup>, and Masruroh<sup>1</sup>

Artikel ini telah dipresentasikan pada kegiatan Seminar Nasional Fisika (Sinafi X) & International Physics Conference (IPC)

Universitas Pendidikan Indonesia, Bandung, Indonesia

9 November 2024

### Abstract

Coating hydroxyapatite (HAp) on stainless steel 316L (SS 316L) by electrochemical deposition method (ECD) was carried out to enhance the biocompatibility and corrosion resistance of metal implants for biomedical applications. One major issue in the ECD process is the water reduction causes an abundance of hydrogen (H<sub>2</sub>) bubbles, which subsequently contribute to forming a porous HAp coating. In this study, the effectiveness of HAp deposition was compared between a direct current (DC) process and a superposition alternating current-direct current (AC-DC) process. The ECD was conducted at pH 6 and 70°C, with the DC process operating at 5 V, while the AC-DC process employed 2.5 V AC and 2.5 V DC at 60 Hz. After deposition, the samples were annealed at 600°C for 2 hours in an argon atmosphere. The corrosion resistance was examined by potentiodynamic polarization. Electrochemical analysis indicated that the AC-DC superposition technique resulted in a significantly higher polarization resistance ( $R_p$ ) of  $4.87 \times 10^4 \Omega/\text{cm}^2$ , compared to the DC sample ( $7.65 \times 10^3 \Omega/\text{cm}^2$ ), with a more positive potential corrosion  $\{[E]_{\text{corr}}\}$  and lower corrosion current density ( $i_{\text{corr}}$ ). The AC-DC techniques minimizing (H<sub>2</sub>) bubbles formation and promoting smoother transition, facilitated the formation of a more homogenous coating and effectively covered substrate surface, thus exhibiting better corrosion resistance. Furthermore, this enhanced corrosion resistance has significant implications for biomedical applications. By prolonging implant lifespan, reducing the release of metal ions like (nickel and chromium), and pitting corrosion in simulated body fluid.

**Keywords** : hydroxyapatite · stainless steel 316L · electrochemical deposition · AC-DC superposition · corrosion resistance

### INTRODUCTION

Austenitic stainless steel 316L (SS 316L) is widely used in metallic materials because of its biocompatibility, good mechanical properties, and low cost (Gopi et al., 2013). However, despite these advantages, the release of metal ions such as chromium and nickel into the body and pitting corrosion, which can cause allergies, and chronic inflammation, significantly limits the lifespan of

✉ Alivia Nurul Avivin  
[Alivianurul5@gmail.com](mailto:Alivianurul5@gmail.com)

<sup>1</sup> Universitas Brawijaya. Malang, Indonesia.

<sup>2</sup> Research Center for Advanced Materials, National Research and Innovation Agency (BRIN). South Tangerang, Indonesia.

<sup>3</sup> Universitas Pendidikan Indonesia, Bandung, Indonesia.

SS 316L implant (Kaliaraj et al., 2021). Therefore, creating a stable protection layer on metallic implants is crucial for their long term application (Koumya et al., 2021). Furthermore, hydroxyapatite (HAp) is widely known as a bone substitute or a coating material for implanting due to its bioactivity and osseointegration capabilities, rendering it suitable for bone implant applications (Yan et al., 2017). Various methods have been developed for coating HAp, including plasma spraying, pulsed laser deposition, sol-gel deposition, biomimetic deposition, and electrochemical deposition (ECD) (Sarbjit Kaur et al., 2019). Among these methods, ECD is interesting due to its ability to produce homogenous coatings with controlled deposition parameters (Arul Xavier & U., 2018; Vladescu et al., 2017).

Nevertheless, a critical challenge in the ECD process is water reduction at the cathode, resulting in hydrogen bubbles forming (Gopi et al., 2012; Li et al., 2020). These bubbles interfere with the migration of calcium and phosphate ions, leading to premature precipitation in the bulk solution instead of uniform deposition on the substrate (Gopi et al., 2012). Furthermore, concentration polarization can arise when the ion mobility is lower than the diffusion rate within the bulk electrolyte towards the substrate surface (Dev et al., 2022; Li et al., 2020), resulting in nonhomogeneous coatings and reduced corrosion resistance (Arul Xavier & U., 2018). Several studies have been undertaken to address the limitations above, such as adding  $H_2O_2$  to the electrolyte (Thanh et al., 2013) and using pulsed current during the ECD process (Dhiflaoui et al., 2024; Gopi et al., 2012). Some researchers have reported that during the pulsed ECD process, the off-pulsed periods play a crucial role in optimizing deposition. The off-pulse time allows hydrogen gas bubbles to detach from the substrate surface, and replenish ions at the electrode surface, which subsequently reduces the concentration polarization (Gopi et al., 2012; Li et al., 2020). However, when pulsed ECD is applied with abrupt on-off voltage transitions, the nucleation rate of HAp becomes unstable due to voltage fluctuation.

This study explores the use of superposition of alternating current-direct current (AC-DC) during the ECD process to overcome this limitation. In superimposed AC-DC condition, characterized by its periodic reversal of direction, can effectively reduce concentration polarization at the cathode (Chávez-Valdez & Boccaccini, 2012; Srimathi et al., 1982). Unlike pulsed current, the sinusoidal waveform by the AC voltage improves smoother voltage transitions (Lete et al., 2019), which reduces internal stress in the deposited layer (Kovac, 1971). This stabilization results in more uniform and orderly nucleations of HAp coating. Previous studies highlight that by combining an AC component with DC, the superposition mechanism is expected to improve ion mobility (Chávez-Valdez & Boccaccini, 2012), reduce hydrogen bubble adherence (Kovac, 1971), and enhance the HAp layer's uniformity (Chipman et al., 2024). This combination of smoother transitions and improved ion transport makes AC-DC techniques (Srimathi et al., 1982) a promising alternative to address the limitation of conventional DC and Pulsed ECD. To the best of our knowledge, coating HAp on the SS 316L substrate via ECD using a combination of AC-DC techniques has not been reported. This novel approach intends to increase coating homogeneity, and corrosion resistance for long-term bioimplant applications.

## MATERIALS AND METHODS

### Sample Preparation

Commercial SS 316L plates with dimensions of (30 x 15 x 3) mm<sup>3</sup> were used as substrates for electrochemical deposition. The substrate was polished with SiC emery papers ranging from (P120 to P1500 grit), followed by ultrasonic cleaning with ethanol and water for 10 min. Then, to improve the surface roughness, the polished substrate was subjected to an acid etching treatment with a mixture of hydrochloric acid (37%), nitric acid (65%), phosphoric acid (85%), and distilled water in the volume ratio of 3:1:1:5. After the etching process, the substrates were rinsed with ethanol and distilled water by ultrasonic cleaner for 10 min and then dried at room temperature.

### Electrolyte Solutions Preparation

The various parameters is a main crucial for reproducibility on the ECD process, and the parameter's of this process were adapted from ref (Gopi et al., 2012; Puranto et al., 2024). Specifically, the ECD process of calcium phosphate coating (CaP) on SS 316L substrate was carried out in an aqueous solution of 0.042 M ( $Ca(NO_3)_2 \cdot 4H_2O$ ) and 0.025 M ( $(NH_4)_2HPO_4$ ). All the reagents were of analytical grade, and the solution was adjusted to have pH 6. The deposition process was carried out by placing the SS 316L and Pt as working electrode (cathode) and counter electrode (anode), respectively. The distance between the two electrodes was kept at 2 cm away (as illustrated in Figure 1). The ECD was conducted by immersing the electrodes in the electrolyte while magnetically stirring and applying a constant DC voltage of 5 V for 1 h at 70 °C. Meanwhile, the AC-DC sample was synthesized by applying 2.5 V AC and 2.5 V DC at 60 Hz. After ECD, the coated sample was removed from the electrolyte, rinsed with ethanol, and dried at room temperature. Then, to obtain most of the HAp phase, the samples were annealed at 600 °C for 2 hours in an argon atmosphere (Puranto et al., 2024).

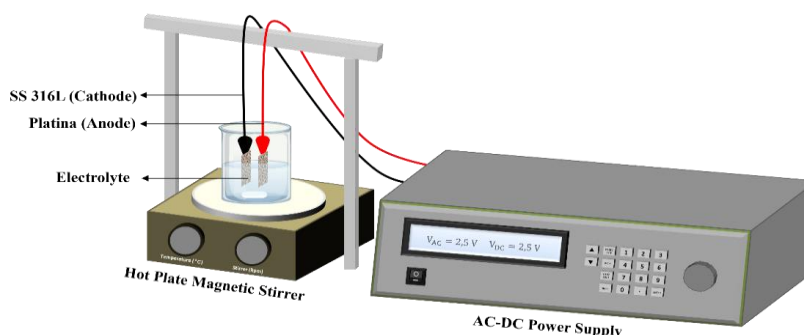


**Figure 1.** Schematic of the ECD process

### Corrosion test by electrochemical testing

The corrosion test was carried out by potentiostat Parstat 4000A. In this research, the sample was placed as the working electrode, platinum was the counter electrode, and Ag/AgCl was the reference electrode in the Ringer medium. The composition of Ringer solution: NaCl 8.69 g/l, KCl 0.30 g/l, CaCl<sub>2</sub> 0,48 g/l was adjusted in pH 6.4. To stabilize the open circuit potential (OCP), the samples were immersed in the Ringer solution for 30 min. The polarization curve was obtained in the scanning range of -0.5 V to +0.5 V at a rate of 5 mV/s with a step potential

of 1 mV. The obtained polarization curve was analyzed using Ameteksi VersaStudio software to extract the polarization parameters such as corrosion potential ( $E_{corr}$ ), corrosion current density ( $i_{corr}$ ), the slopes of anodic ( $\beta_a$ ), and cathodic ( $\beta_c$ ) branches using the Tafel extrapolation method. The electrochemical performances of the deposited coating were calculated according to the Stern-Geary equation:

$$i_{corr} = \frac{\beta_a \beta_c}{2.303(\beta_a + \beta_c)} \frac{1}{R_p} \quad (1)$$

## RESULTS AND DISCUSSION

### Electrochemical Corrosion

Corrosion in metal implants is a significant challenge in biomedical applications (Koumya et al., 2021). When a metal implant comes into direct contact with the human body, which contains chloride, proteins, and amino acids, along with reduced oxygen concentration, these conditions may interrupt the creation of a protective oxide layer on the implant surface, promoting corrosion. As a result, metal ions (such as nickel and chromium) can be released, causing toxicity (Nizami et al., 2022). This can create a variety of issues, including the release of metal ions into the body, which can cause allergies, tissue atrophy, and chronic inflammation (Koumya et al., 2021). Corrosion occurs when the metal substrate (SS 316L) undergoes exposure to an electrolyte, initiating electrochemical reactions (Voisin et al., 2022). In the Ringer solution, the chloride ions ( $Cl^-$ ) aggressively attack the passive oxide layer ( $Cr_2O_3$ ) on the SS 316L surface, indicating the initiation of pitting corrosion (Naghbi et al., 2014). The chemical reaction in anodic sites:



Meanwhile, at the cathodic sites, a reduction occurs, often involving oxygen and water:



It should be noted that chloride ions in the solution often initiate pitting corrosion at the SS 316L surface. Aggressive  $Cl^-$  ions enhanced the dissolution of  $Fe^{2+}$  by forming soluble  $FeCl_3$ , leading to substrate degradation (Gopi et al., 2009). The HAp coating acts as a protective barrier, minimizing the substrate's exposure to the electrolyte and preventing metal ions dissolution, thereby decelerating the corrosion process (Gopi, Ramya, et al., 2013). Therefore, in this study, the corrosion resistance property of the coating through electrochemical deposition was evaluated by polarization studies and shown in Figure 2.

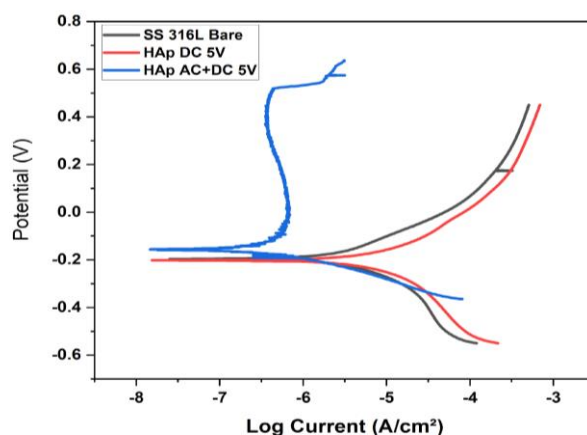


**Figure 2.** Polarization curve of bare SS 316L and HAp-coated samples using DC and AC-DC voltage in Ringer's solution.

The electrochemical property was evaluated through polarization studies, with the results obtained for pristine and HAp coated on SS 316L at different voltage techniques as presented in Figure 2. As can be observed, the polarization curve for HAp-coated samples exhibited a more positive  $E_{corr}$  compared to pristine SS 316L ( $-1.88 \times 10^{-1} V$ ). Specifically,  $E_{corr}$  increased to  $-1.53 \times 10^{-1} V$  for samples coated under AC-DC superposition, indicating better corrosion resistance. Conversely, for the HAp-coated specimen at DC voltage, a shift in potential toward the active direction  $-2.01 \times 10^{-1} V$  was observed, suggesting less effective corrosion protection. Furthermore, the sample coated under AC-DC voltage exhibited the lowest  $i_{corr}$  values at  $2.6 \times 10^{-7} A/cm^2$  compared to the other samples. This was followed by sample DC 5V and pristine SS 316L, with  $i_{corr}$  value is  $3.5 \times 10^{-6} A/cm^2$ , and  $4.8 \times 10^{-5} A/cm^2$  respectively. The lower of  $i_{corr}$  values indicate a significant reduction in the corrosion rate, inferring that the deposition mechanism using a combination of AC-DC voltage produces a more effective protective layer.

Surprisingly, the polarization curve of the AC-DC sample show more positive  $E_{corr}$  and lower  $i_{corr}$  compared to the other sample. Furthermore, it demonstrated the highest  $R_p$  values among all tested samples, which measures  $4.87 \times 10^4 \Omega/cm^2$ . These findings show that the HAp layer deposited under AC-DC voltage was nobler than the DC deposited layer due to a more homogeneous structure and better substrate coverage, thus exhibiting better corrosion resistance. This improvement is attributed to the fact that under the AC-DC voltage combination, the nucleation rate and crystal growth occur in a consistent and controlled manner. Additionally, when the voltage approaches zero,  $H_2$  bubbles can escape from the metal substrate during the ECD process. That minimum amount of  $H_2$  at the metal-electrolyte interface produces a non-porous HAp layer. In contrast, the HAp-coated sample under DC voltage and the bare SS 316L sample show corrosion susceptibility. The thin and porous coating for the DC sample is less effective in protecting the substrate in a corrosive environment. During the electrochemical deposition process with DC voltage, the process occurs constantly and continuously, leaving no opportunity for  $H_2$  gas to escape from the substrate, resulting in a porous coating. The corrosion test parameters are shown in Table 1.

**Table 1.** Corrosion parameters derived from polarization curves.

Sample	Corrosion parameter from Tafel curve				
	$i_{corr} (\frac{A}{cm^2})$	$E_{corr} (V)$	$\beta_a (mV)$	$\beta_c (mV)$	$R_p (\frac{\Omega}{cm^2})$
SS 316L	$4.8 \times 10^{-5}$	$-1.88 \times 10^{-1}$	$2.32 \times 10^{-1}$	$2.32 \times 10^{-1}$	$1.05 \times 10^3$
DC 5V	$3.5 \times 10^{-6}$	$-2.01 \times 10^{-1}$	$8 \times 10^{-2}$	$9.7 \times 10^{-2}$	$7.65 \times 10^3$
AC+DC 5Vpp	$2.6 \times 10^{-7}$	$-1.53 \times 10^{-1}$	$1.3 \times 10^{-1}$	$8.6 \times 10^{-1}$	$4.87 \times 10^4$

The corrosion resistance behavior of HAp coatings on SS 316L derived from various conditions on ECD process are compared (Stango & Vijayalakshmi, 2021; Chakraborty et al., 2016; Prasad et al., 2023) to examine the novelty of the deposition technique. The results, presented in Table 2, demonstrate that the AC-DC superposition method resulted in coating with significantly higher polarization resistance values, more positive  $E_{corr}$ , and lower  $i_{corr}$  value compared to other methods. For example, Stago et al. (Arul Xavier Stango & Vijayalakshmi, 2021) reported a polarization resistance value for ECD with DC voltage at -1.5 V, similar to those obtained by Chakraborty et al. (Chakraborty et al., 2016) using pulsed ECD. This improvement is ascribed to the coating's increased homogeneity, which covers the substrate and protects it from the corrosive environment. In fact, these results are significant for biomedical applications, where the metallic implants are subjected to extreme conditions that include proteins, amino acids, and chloride ions. The AC-DC deposition techniques improved corrosion resistance and can prolong implant life, lower the release of harmful metal ions like nickel and chromium, and lower the patient's chance of developing chronic inflammation and other adverse effects.

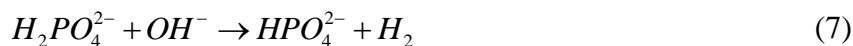
**Table 2.** Comparative study for corrosion resistance of HAp coated in SS 316L from various voltage techniques based on literature

Sampel Condition		Corrosion Parameter			Ref
Methods	Parameter	$E_{corr} (V)$	$i_{corr} (\frac{A}{cm^2})$	$R_p (\frac{\Omega}{cm^2})$	
ECD (DC Voltage)	$V_{DC} = 5 V$	$-2.07 \times 10^{-1}$	$3.5 \times 10^{-6}$	$7.65 \times 10^3$	Present work
ECD (AC-DC Voltage)	$V_{AC} = 2.5 V$ dan $V_{DC} = 2.5 V$	$-1.53 \times 10^{-1}$	$2.6 \times 10^{-7}$	$4.87 \times 10^4$	Present work
ECD (DC Voltage)	$V_{DC} = -1.5 V$	$-2.5 \times 10^{-1}$	$1.1 \times 10^{-6}$	$2.4 \times 10^4$	Puranto et al. 2024
PED (Galvanostatic)	$i = 5 mA/cm^2$	$-3.78 \times 10^{-1}$	$2.19 \times 10^{-6}$	$2.4 \times 10^4$	Safavi et al. 2021
PED (Galvanostatic)	$i = 50 mA/cm^2$	$-3.25 \times 10^{-1}$	$1.58 \times 10^{-5}$	—	Kaur et al. 2019

### Mechanism of electrochemical deposition

The electrochemical reaction that occurs during ECD is presented in equation 3-7 (Safavi et al., 2021).





At the working electrode,  $H_2O$  and  $H^+$  undergo reduction reaction, yielding hydrogen gas and hydroxyl ions (Eq. 4-5). Hydrogen gas also resulted from the reaction of  $OH^-$  and phosphate species (Eq. 6-7), which contradicts ECD HAp coating in term reaction efficiency and coating quality. When the voltage or current densities increase, hydroxide production can accelerate (Djošić et al., 2021). This can lead to excessive hydrogen gas evolution during the ECD process (Gopi et al., 2012). Furthermore, the higher current densities in ECD process in DC voltage, concentration polarization occurs in the cathode surface. This arises from the diffusion layer between bulk electrolyte and cathode surface, creating a gradient concentration that hinders the transport of ions and replenishes ions at the electrode surface. This problem is consistent with finding in previous studies that hydrogen bubbles and polarization concentration will inhibit the deposition of HAp, resulting in a porous coating (Arul Xavier Stango & Vijayalakshmi, 2021; Gopi et al., 2012; Li et al., 2020; Prasad et al., 2023).

The pulsed method was applied during ECD to overcome the drawback mentioned above. In the pulsed ECD method, the electrical current is applied in on/off cycles to reduce hydrogen gas accumulation (Chakraborty et al., 2016; Gopi et al., 2012; Prasad et al., 2023). Gopi et al. reported that the pulsed ECD method approach on SS 316L substrate allows for longer relaxation periods, enabling hydrogen gas to detach from the substrate surface and provide a more homogeneous coating (Gopi et al., 2012). However, this method is applied with abrupt on-off voltage transitions (Dev et al., 2022), lead to instability in the nucleation of HAp. As an alternative, an AC-DC voltage combination can be applied. The sinusoidal waveform from the AC voltage is generated from this combination, generating appropriate smoother voltage transitions (Srimathi et al., 1982) and reducing internal stress within the deposited layer's (Kovac, 1971). Additionally, when the voltage approaches zero,  $H_2$  gas formed can escape from the Ca-P layer during the ECD process, further enhancing the coating quality.

The mechanism of ECD is illustrated in Figure 3. Figure 3(a) and 3(b) demonstrates the ECD process with DC voltage, where the continuous and constant current application leads to  $H_2$  gas to escape from the substrate, resulting in a porous coating. In contrast, Figure 3(c) and 3(d) illustrated the AC-DC superposition method. The sinusoidal waveform from the AC voltage by this combination, resulting in suitable smoother voltage transitions that can successfully lessen concentration polarization at the cathode. Furthermore, the  $H_2$  gas produced during the ECD process can escape the Ca-P layer as the voltage near closer to zero, improving the coating quality even more. On the other hand, the AC-DC superposition also induces periodic fluctuations in the cathode potential, leading to change in ion concentration. These fluctuations shift the potential towards more positive values (Abd El-Halim et al., 1984). This reduces ion depletion on the cathode surface, resulting in steady ion migration and homogeneous coating deposition (Vijayavalli et al., 1963). Furthermore, periodic fluctuations

influenced by electrical solution properties, including ohmic and capacitive components, have a direct impact on deposition rates and coating quality (Abd El Rehim et al., 1984; Sheshadri et al., 1981). These findings deepen our understanding of the role of electrical parameters in optimizing reaction kinetics and deposition processes. The homogeneous coating produced by the AC-DC method approach demonstrated superior corrosion resistance compared to DC methods. Despite these advances, scaling up AC-DC superposition for industry presents challenges. Including precise control of parameters like frequency and amplitude remains critical in scaling up, which requires advanced equipment and optimized equipment use. Addressing these challenges could facilitate broader applications in biomedical implant manufacturing, improving coating homogeneity, reducing patient risks, and extending implant lifetimes.

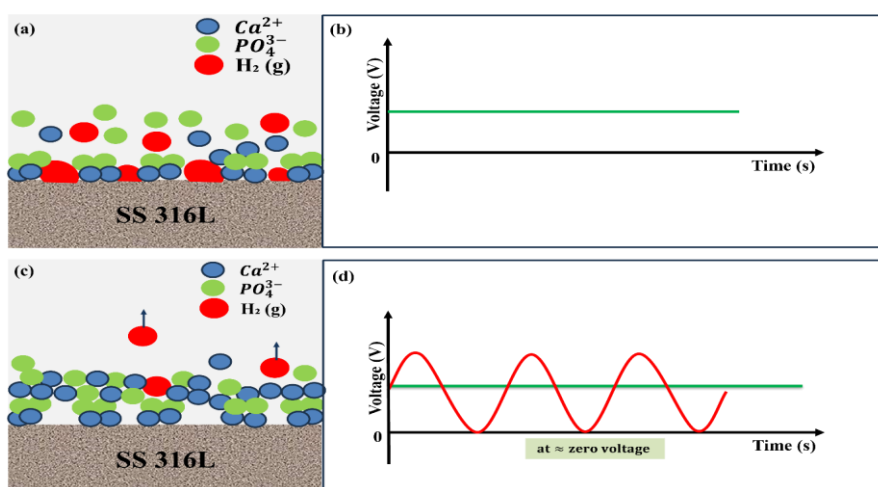


**Figure 3.** Schematic process when (a) During on DC voltage, (b) Waveform of DC voltage (c) During on AC-DC voltage applied near to zero, (d) Waveform of superimposed AC-DC voltage

## CONCLUSION

The coating of HAp on stainless steel 316L has been effectively achieved by utilizing two different techniques. The electrochemical analysis indicated that the  $E_{corr}$  value of the AC-DC samples was more positive than that of the DC sample, and the  $i_{corr}$  value was lower compared to the DC sample, demonstrating better corrosion resistance. The polarization resistance of the AC-DC sample was  $4.87 \times 10^4 \Omega/cm^2$ , higher than the  $7.65 \times 10^3 \Omega/cm^2$  observed with the DC process. Additionally, the significant improvement in corrosion resistance for the AC-DC coated layer was evidenced by a reduction in corrosion current, indicating more effective corrosion protection. The AC-DC superposition mechanism facilitated smoother ion movement and minimized hydrogen bubble adherence, resulting in a more homogeneous coating. This enhanced quality of the layer contributed to its superior corrosion resistance and long-term performance in biomedical applications.

## REFERENCES

- Abd El Rehim, S. S., Abd El-Halim, A. M., & Osman, M. M. (1984). The effect of superimposing an a.c. on d.c. the electrodeposition of Co-Ni alloys from a Watts plating bath. *Surface Technology*, 22(4), 337–342. [https://doi.org/10.1016/0376-4583\(84\)90097-9](https://doi.org/10.1016/0376-4583(84)90097-9)



- Abd El-Halim, A. M., Baghlaf, A. O., & Sobahi, M. I. (1984). Influence of a superimposed a.c. on cadmium electroplating from an acidic chloride bath. *Surface Technology*, 22(2), 143–154. [https://doi.org/10.1016/0376-4583\(84\)90050-5](https://doi.org/10.1016/0376-4583(84)90050-5)
- Arul Xavier, S., & U., V. (2018). Electrochemically grown functionalized -Multi-walled carbon nanotubes/hydroxyapatite hybrids on surgical grade 316L SS with enhanced corrosion resistance and bioactivity. *Colloids and Surfaces B: Biointerfaces*, 171, 186–196. <https://doi.org/10.1016/j.colsurfb.2018.06.058>
- Arul Xavier Stango, S., & Vijayalakshmi, U. (2021). Electrochemical deposition of HAP/f-MWCNTs and HAP/GO composite layers on 316L SS implant with excellent corrosion resistance performance. *Materials Letters*, 304, 130666. <https://doi.org/10.1016/j.matlet.2021.130666>
- Chakraborty, R., Sengupta, S., Saha, P., Das, K., & Das, S. (2016). Synthesis of calcium hydrogen phosphate and hydroxyapatite coating on SS316 substrate through pulsed electrodeposition. *Materials Science and Engineering: C*, 69, 875–883. <https://doi.org/10.1016/j.msec.2016.07.044>
- Chávez-Valdez, A., & Boccaccini, A. R. (2012). Innovations in electrophoretic deposition: Alternating current and pulsed direct current methods. *Electrochimica Acta*, 65, 70–89. <https://doi.org/10.1016/j.electacta.2012.01.015>
- Chipman, G., Johnson, B., & Rappleye, D. (2024). Application of AC superimposed DC waveforms to bismuth electrorefining. *Nuclear Engineering and Technology*, 56(4), 1339–1346. <https://doi.org/10.1016/j.net.2023.11.038>
- Dev, P. R., Anand, C. P., Michael, D. S., & Wilson, P. (2022). Hydroxyapatite coatings: a critical review on electrodeposition parametric variations influencing crystal facet orientation towards enhanced electrochemical sensing. *Materials Advances*, 3(21), 7773–7809. <https://doi.org/10.1039/D2MA00620K>
- Dhiflaoui, H., Dabaki, Y., Zayani, W., Debbich, H., Faure, J., Larbi, A. B. C., & Benhayoune, H. (2024). Effects of Hydrogen Peroxide Concentration and Heat Treatment on the Mechanical Characteristics and Corrosion Resistance of Hydroxyapatite Coatings. *Journal of Materials Engineering and Performance*, 33(5), 2104–2115. <https://doi.org/10.1007/s11665-023-08132-9>
- Djošić, M., Janković, A., & Mišković-Stanković, V. (2021). Electrophoretic Deposition of Biocompatible and Bioactive Hydroxyapatite-Based Coatings on Titanium. *Materials*, 14(18), 5391. <https://doi.org/10.3390/ma14185391>
- Gopi, D., Indira, J., & Kavitha, L. (2012). A comparative study on the direct and pulsed current electrodeposition of hydroxyapatite coatings on surgical grade stainless steel. *Surface and Coatings Technology*, 206(11–12), 2859–2869. <https://doi.org/10.1016/j.surfcoat.2011.12.011>
- Gopi, D., Prakash, V. C. A., & Kavitha, L. (2009). Evaluation of hydroxyapatite coatings on borate passivated 316L SS in Ringer's solution. *Materials Science and Engineering: C*, 29(3), 955–958. <https://doi.org/10.1016/j.msec.2008.08.020>
- Gopi, D., Rajeswari, D., Ramya, S., Sekar, M., R, P., Dwivedi, J., Kavitha, L., & Ramaseshan, R. (2013). Enhanced corrosion resistance of strontium hydroxyapatite coating on electron beam treated surgical grade stainless steel. *Applied Surface Science*, 286, 83–90. <https://doi.org/10.1016/j.apsusc.2013.09.023>
- Gopi, D., Ramya, S., Rajeswari, D., & Kavitha, L. (2013). Corrosion protection performance of porous strontium hydroxyapatite coating on polypyrrole coated 316L stainless steel. *Colloids and Surfaces B: Biointerfaces*, 107, 130–136. <https://doi.org/10.1016/j.colsurfb.2013.01.065>
- Kaliaraj, G. S., Siva, T., & Ramadoss, A. (2021). Surface functionalized bioceramics coated on metallic implants for biomedical and anticorrosion performance – a review. *Journal of Materials Chemistry B*, 9(46), 9433–9460. <https://doi.org/10.1039/D1TB01301G>
- Koumya, Y., Ait Salam, Y., Khadiri, M. E., Benzakour, J., Romane, A., Abouelfida, A., & Benyaich, A. (2021). Pitting corrosion behavior of SS-316L in simulated body fluid and electrochemically assisted deposition of hydroxyapatite coating. *Chemical Papers*, 75(6), 2667–2682. <https://doi.org/10.1007/s11696-021-01517-x>

- Kovac, Z. (1971). The Effect of Superimposed A.C. on D.C. in Electrodeposition of Ni-Fe Alloys. *Journal of The Electrochemical Society*, 118(1), 51. <https://doi.org/10.1149/1.2407950>
- Lete, C., Marin, M., Anghel, E. M., Preda, L., Matei, C., & Lupu, S. (2019). Sinusoidal voltage electrodeposition of PEDOT-Prussian blue nanoparticles composite and its application to amperometric sensing of H<sub>2</sub>O<sub>2</sub> in human blood. *Materials Science and Engineering: C*, 102, 661–669. <https://doi.org/10.1016/j.msec.2019.04.086>
- Li, T.-T., Ling, L., Lin, M.-C., Peng, H.-K., Ren, H.-T., Lou, C.-W., & Lin, J.-H. (2020). Recent advances in multifunctional hydroxyapatite coating by electrochemical deposition. *Journal of Materials Science*, 55(15), 6352–6374. <https://doi.org/10.1007/s10853-020-04467-z>
- Naghibi, S. A., Raeissi, K., & Fathi, M. H. (2014). Corrosion and tribocorrosion behavior of Ti/TiN PVD coating on 316L stainless steel substrate in Ringer's solution. *Materials Chemistry and Physics*, 148(3), 614–623. <https://doi.org/10.1016/j.matchemphys.2014.08.025>
- Nizami, M. Z. I., Campéon, B. D. L., & Nishina, Y. (2022). Electrodeposition of hydroxyapatite and graphene oxide improves the bioactivity of medical grade stainless steel. *Materials Today Sustainability*, 19, 100193. <https://doi.org/10.1016/j.mtsust.2022.100193>
- Prasad, P. S., Hazra, C., Jena, S., Byram, P. K., Sen, R., Chakravorty, N., Das, S., & Das, K. (2023). Pulse galvanostatic electrodeposition of biosurfactant assisted brushite-hydroxyapatite coatings on 316 L stainless steel with enhanced electrochemical and biological properties. *Colloids and Surfaces A: Physicochemical and Engineering Aspects*, 671, 131651. <https://doi.org/10.1016/j.colsurfa.2023.131651>
- Puranto, P., Kamil, M. P., Suwondo, K. P., Mellinia, A. D., Avivin, A. N., Ulfah, I. M., Fitriani, D. A., Azahra, S. A., Hanafi, R., Saudi, A. U., Masruroh, & Kozin, M. (2024). Unveiling the pH influence: Enhancing hydroxyapatite-coated titanium biomedical implants through electrochemical deposition. *Ceramics International*, 50(8), 13412–13421. <https://doi.org/10.1016/j.ceramint.2024.01.253>
- Safavi, M. S., Walsh, F. C., Surmeneva, M. A., Surmenev, R. A., & Khalil-Allafi, J. (2021). Electrodeposited Hydroxyapatite-Based Biocoatings: Recent Progress and Future Challenges. *Coatings*, 11(1), 110. <https://doi.org/10.3390/coatings11010110>
- Sarbjit, Bala, N., & Khosla, C. (2019). Characterization of Hydroxyapatite Coating on 316L Stainless Steel by Sol–Gel Technique. *Surface Engineering and Applied Electrochemistry*, 55(3), 357–366. <https://doi.org/10.3103/S1068375519030104>
- Sheshadri, B. S., Koppa, V., Jai Prakash, B. S., & Mayanna, S. M. (1981). The effect of the superposition of an alternating current on a direct current on the electrodeposition of Ni-Fe alloys. *Surface Technology*, 13(2), 111–117. [https://doi.org/10.1016/0376-4583\(81\)90051-0](https://doi.org/10.1016/0376-4583(81)90051-0)
- Srimathi, S. N., Sheshadri, B. S., & Mayanna, S. M. (1982). Electroplating of thin films of Fe-Ni alloys: Some effects of superimposed alternating current on direct current. *Surface Technology*, 17(3), 217–227. [https://doi.org/10.1016/0376-4583\(82\)90004-8](https://doi.org/10.1016/0376-4583(82)90004-8)
- Thanh, D. T. M., Nam, P. T., Phuong, N. T., Que, L. X., Anh, N. Van, Hoang, T., & Lam, T. D. (2013). Controlling the electrodeposition, morphology and structure of hydroxyapatite coating on 316L stainless steel. *Materials Science and Engineering: C*, 33(4), 2037–2045. <https://doi.org/10.1016/j.msec.2013.01.018>
- Vijayavalli, R., Rao, P. V. V., Sampath, S., & Udupa, H. V. K. (1963). Function of A.C. Superimposed on D.C. in the Anodic Oxidation of Lead in Sulfuric Acid. *Journal of The Electrochemical Society*, 110(1), 1. <https://doi.org/10.1149/1.2425664>
- Vladescu, A., Vranceanu, D. M., Kulesza, S., Ivanov, A. N., Bramowicz, M., Fedonnikov, A. S., Braic, M., Norkin, I. A., Koptuyug, A., Kurtukova, M. O., Dinu, M., Pana, I., Surmeneva, M. A., Surmenev, R. A., & Cotrut, C. M. (2017). Influence of the electrolyte's pH on the properties of electrochemically deposited hydroxyapatite coating on additively manufactured Ti64 alloy. *Scientific Reports*, 7(1), 16819. <https://doi.org/10.1038/s41598-017-16985-z>
- Voisin, T., Shi, R., Zhu, Y., Qi, Z., Wu, M., Sen-Britain, S., Zhang, Y., Qiu, S. R., Wang, Y. M., Thomas, S., & Wood, B. C. (2022). Pitting Corrosion in 316L Stainless Steel Fabricated by Laser

Powder Bed Fusion Additive Manufacturing: A Review and Perspective. *JOM*, 74(4), 1668–1689. <https://doi.org/10.1007/s11837-022-05206-2>

Yan, L., Xiang, Y., Yu, J., Wang, Y., & Cui, W. (2017). Fabrication of Antibacterial and Antiwear Hydroxyapatite Coatings via In Situ Chitosan-Mediated Pulse Electrochemical Deposition. *ACS Applied Materials & Interfaces*, 9(5), 5023–5030. <https://doi.org/10.1021/acsami.6b15979>

